

Supplementary Materials for

Genomic agonism and phenotypic antagonism between estrogen and progesterone receptors in breast cancer

Hari Singhal, Marianne E. Greene, Gerard Tarulli, Allison L. Zarnke, Ryan J. Bourgo, Muriel Laine, Ya-Fang Chang, Shihong Ma, Anna G. Dembo, Ganesh V. Raj, Theresa E. Hickey, Wayne D. Tilley, Geoffrey L. Greene

Published 24 June 2016, *Sci. Adv.* 2, e1501924 (2016)

DOI: 10.1126/sciadv.1501924

The PDF file includes:

- table S1. Clinical information of tumors.
- table S2. PCR primers for ChIP-PCR and reChIP-PCR.
- table S3. PCR primers for CATCH chromosome capture.
- Legends for tables S4 to S6
- table S7. Summaries of patient cohorts.
- fig. S1. Progesterin is a genomic agonist of estrogen-regulated gene expression.
- fig. S2. Progesterin is a phenotypic antagonist of estrogen-induced cell proliferation, invasion, and migration.
- fig. S3. Progesterin modulates estrogen-regulated gene expression.
- fig. S4. PR redirects ER to sites enriched for motifs of PR and PR-associated cofactors.
- fig. S5. Noncompetitive interactions between ER and PR.
- fig. S6. Depletion of FOXA1 or NF1C insignificantly impacts the effects of PR on ER-regulated gene expression.
- fig. S7. PR-regulated genes are enriched for breast cancer signatures, and PR contributes to the prognostic value of ER.

Other Supplementary Material for this manuscript includes the following:

(available at advances.sciencemag.org/cgi/content/full/2/6/e1501924/DC1)

- table S4 (Microsoft Excel format). Gene expression changes observed in eight ER⁺/PR⁺ patient tumors and three ER⁺/PR⁺ cell models in response to various combinations of estrogen and progesterin treatments.

- table S5 (Microsoft Excel format). Gene expression changes observed in four ER⁺/PR⁻ patient tumors and two ER⁺/PR-deficient cell models in response to various combinations of estrogen and progestin treatments.
- table S6 (Microsoft Excel format). Binding sites for ER, PR, and ER/PR complexes in ER⁺/PR⁺ T47D and ER⁺/PR-deficient T47D cells.

table S1. Clinical information of tumors					Regulation by E2		
Tumor ID	Treatment time	Age	Receptor Status	Diagnosis	GREB1	PR	E2F1
P1	24 hrs	61	ER+ PR+ HER2+	Invasive carcinoma of micropapillary type.	No	1.2 fold	No
P2	24 hrs	64	ER+ PR+ HER2-	Invasive carcinoma of no special type.	1.8 fold	No	1.4 fold
P3	24 hrs	52	ER+ PR+ HER2-	IDC	1.7 fold	2.5 fold	2.78 fold
P4	48 hrs	53	ER+ (90%) PR+ (75%) Her2-	IDC			
P5	48 hrs	55	ER+ (98%) PR+ (57%) Her2-	IDC			
P6	48 hrs	63	ER+ (100%) PR+ (95%) Her2-	IDC			
P7	24 hrs	78	ER+ PR+ HER2+/-	Infiltrating ductal carcinoma (IDC)	3 fold	1.2 fold	1.9 fold
P8	24 hrs	39	ER+ PR+ HER2+/-	IDC with focal invasive micropapillary carcinoma.	2 fold	no	no
N1	24 hrs	47	ER+ PR- HER2-	IDC	2 fold	1.5 fold	1.8 fold
N2	48 hrs	54	ER+ PR-Her2-	IDC			
N3	48 hrs	74	ER+ PR-Her2-	IDC			
N4	24 hrs	48	ER+ PR- HER2-	Invasive carcinoma	1.5 fold	1.5 fold	1.2 fold

table S1. Table presents the clinical information of twelve primary tumors used in this study. All the twelve tumors are positive for ER and eight of those are ER+/PR+ (P1 to P8) and four are ER+/PR- (N1 to N4). RNA-seq was performed on tumors treated *ex-vivo* with vehicle, E, P or E+P for 24 or 48 hours.

table S2A. PCR primers for CHIP-PCR.

Gene near binding site	Forward primer	Reverse primer
E2F1	GGTGAGATGGGAGTCTGAGG	GGTGCCTGCAAAGTAGGTTC
FOXA1	TGAGGACTGCTTGGTCACAG	CACCAGCCTTTCCAACCTAA
FOS	CCACTCTGGGCAGATCAGTT	CTGGCTAGATCAGGCTTTGG
GATA3	GCCAAAACCTACCAGCAAAT	TCAGCACCATGCACAAGAAT
TFF1 - binding1	CAGGTCTCGGTTCTCTTTGC	GGGCTATAACCACTTGCCAGA
KLF9 - binding1	GGCTTGAAACCAGAATGTC	CAGTGCTGGGACCAAGAAAG
GREB1	GCTCGCTTATGTGGCTTAGG	CGCTGTGCAAAGAACAAAGG
FHL2 - PR	CGCATTCTCTCAGGACAACC	TCCACTCTACACCAGCCTGA
FHL2 – ER	AGACCGCCCTATGTTTCGTTA	CAAGGTTTGAGTGGGAGGAA
PDZK1 – PR	GACCCCTCATCTGGGAAAAG	GCCTGAGGATCCTTGGAGAG
PDZK1 – ER	TGAGGAAGCTGCTCAATGTC	CCACACTGGAAGAGCCATTT
ESR1 - Enhancer	TGTAGGCTAGTTTTGTTTAACGATTTTT	GGTGATGGGAGAATTGCTTAGAA
ESR2	CTCCGTGGAGCACATAATCC	TGGCTAACCTCCTGATGCTC
CYP26A1	CAGCCTCCCCTGGAATGTA	GCACCATGTAAGCTGGAGAA
FKBP5	AACACCCTGTTCTGAATGTGG	GCATGGTTTAGGGTTCTTG
Control R18s	GAGTGTTCAAAGCAGGTCCAA	CCTCTAGCGGTGCAATACAAA

table S2B. PCR primers for reCHIP-PCR.

Gene	Forward primer	Reverse primer	Chromosome location
E2F1	GGACTGTATGCCTCGTGCTA	CTTGGGTCCCTAAGCTCTGA	chr20:32,291,053-321,971
FOXA1	GGTTTCCGAGGAAGGGATTA	CCCGGGACCTAAAAGTCAA	chr14:38,048,757-074,325
FOS	CAGAGAGATGTTGGCTCAGG	CCGATTCTGGAACAGCTTCT	chr14:75,719,239-742,695
GREB1	CCTATGCAGTTTTGCTGCTG	GCCTACCACAAGGTCAGCTC	chr2:11,617,820-701,367

table S2. PCR primers for CHIP-PCR and reCHIP-PCR. (A) Primers used for directed CHIP-qPCR. **(B)** Primers used for directed reCHIP-qPCR.

table S3. PCR Primers for CATCH chromosome capture.

Oligo Name	Sequence 5' to 3'	Product Size	Internal Oligo	bp DNA Target
CHR21F	GGCTTGTTTGAGAGAGCGAG	100	(chromosome 21)	n/a
CHR21R	TTAACATTGCCCTTGTGCC			
PDZK1 EREF	gggattgcGATGAACTCAGG	123	/5BioTinTEG/TGAAAGA TATAGAGGAGGCCAGGAG	158
PDZK1 ERER	ACCAGCTTATCTTCCTCCACC			
PDZK1 PREF	CAGAGTACACAGTCGCCTCT	111	/5BioTinTEG/AGAGTGG AAAGGGAGACTGTCATAA	159
PDZK1 PRER	GCTCCAGTGGTTTTCTCTCC			
PDZK1 R1F	TGCTGGCTTAATGTTGCACA	111	(chromosome 1 near PRE)	n/a
PDZK1 R1R	TGTTCTTGCAGCACTTGTGT			
PDZK1 R2F	tggactcaagcattcctccc	118	(chromosome 1 near ERE)	n/a
PDZK1 R2R	AGCAATCTGGTCAGGAAGCT			
FHL2 EREF	GTCTAGCCCACCAGCCTC	129	/5BioTinTEG/CTAGAAGCC CTGCCTTTCTTTGG	175
FHL2 ERER	GGGTCTGAGCTGTACAAATGC			
FHL2 PREF	CTGAGAGAAACGTTGCGGAG	108	/5BioTinTEG/CCAGGGAAT GATGCCGAGATAAC	193
FHL2 PRER	CAAAGACAGAGTGCCTTCCA			
FHL2 R1F	AAACCCACCCTTCTGTCCTC	105	(chromosome 2 between ERE/PRE)	n/a
FHL2 R1R	GCTGGACCCTGAGAATGTGA			
FHL2 R2F	CCCTGATCCACCACTGAAGT	109	(chromosome 2 between ERE/PRE)	n/a
FHL2 R2R	GTGGGCAGAGATCACATTCCG			
FHL2 R3F	ACACCAGCTATTCCTGTGGT	110	(chromosome 2 between ERE/PRE)	n/a
FHL2 R3R	CGCAGTGTGAATAAGCAGCA			
FHL2 ERE2F	TGAGAGCCAGACGTTTCAGT	105	(intron 3 of FHL2)	n/a
FHL2 ERE2R	GCTGAGCTTTAGTGGCAAGT			

table S3. PCR primers for CATCH chromosome capture. Primers used for targeted chromosome capture (CATCH) experiments.

tables S4 and S5 (Excel data set files). Tables providing the gene expression observed in response to treatments with either estrogen or progestin or the combination of both the hormones. **Table S4** contains data for eight ER⁺/PR⁺ tumors and three cell models. **Table S5** contains data for four ER⁺/PR⁻ tumors and two PR-deficient cell models. Each of the model system has four treatments conditions.

table S6 (Excel data set files). Binding sites for ER, PR, and ER/PR complexes in ER⁺/PR⁺ T47D and ER⁺/PR-deficient T47D cells. All the binding sites have been annotated using the CHIPSeeker R package.

table S7. Summaries of patient cohorts.				
	METABRIC	METABRIC PR+ group	METABRIC PR- group	TCGA
Grade				
I	170	166	4	101
II	775	712	63	432
III	952	568	384	417
Stage				
I	791	647	144	171
II	447	429	18	583
III	250	33	217	232
IV	486	402	84	17
ER				
Positive	1505	1432	73	754
Negative	435	54	381	222
PR				
Positive	1512	1512	NA	656
Negative	469	NA	469	317
Her2				
Positive	1044	1024	20	150
Negative	937	488	449	527
Pam50 subtype				
Luminal A	708	704	4	434
Luminal B	470	470	0	194
Her2+	228	98	130	67
Basal-like	303	38	265	142
Normal-like	198	161	37	119

table S7. Summaries of patient cohorts. Table summarizing the number of patients in each of the cohorts used in the study (numbers in each stage, grade, subtype, ER, PR and Her2 status)

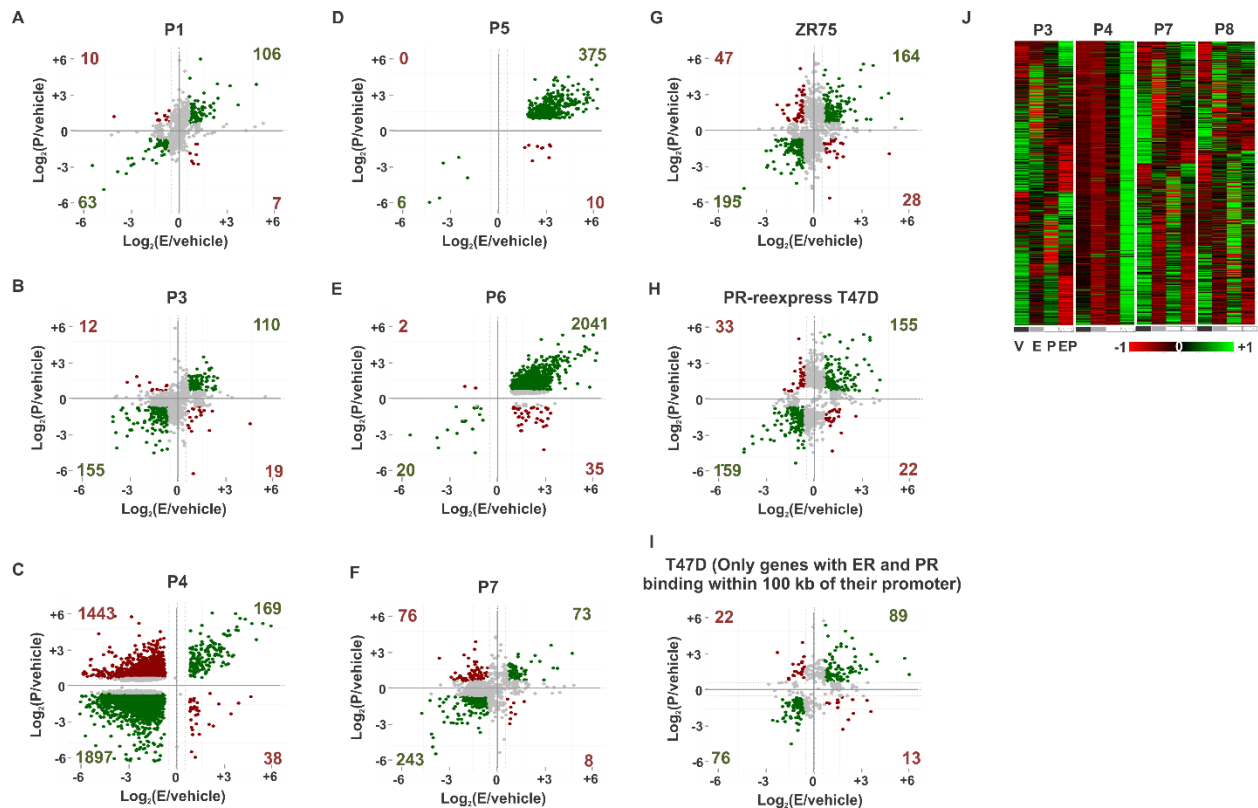


fig. S1. Progestin is a genomic agonist of estrogen-regulated gene expression. (A - I) PR is a genomic agonist of ER-regulated gene expression. Axes in the dot plots denote log fold change of gene expression in **(A - F)** ER+/PR+ patient tumors and **(G - H)** ZR75 and PR re-express T47D cells in response to E or P treatment relative to vehicle. **(I)** For T47D cells, dot plot represents genes that have ER and PR binding within 100kb of their promoters. **(J)** Expression of estrogen and progestin-regulated genes in four ER+/PR+ patient tumors treated ex-vivo with vehicle (V), estrogen (E), progestin R5020 (P) or concomitantly with both hormones (E+P). All heatmaps are row-normalized and include the union of ER and PR-regulated genes.

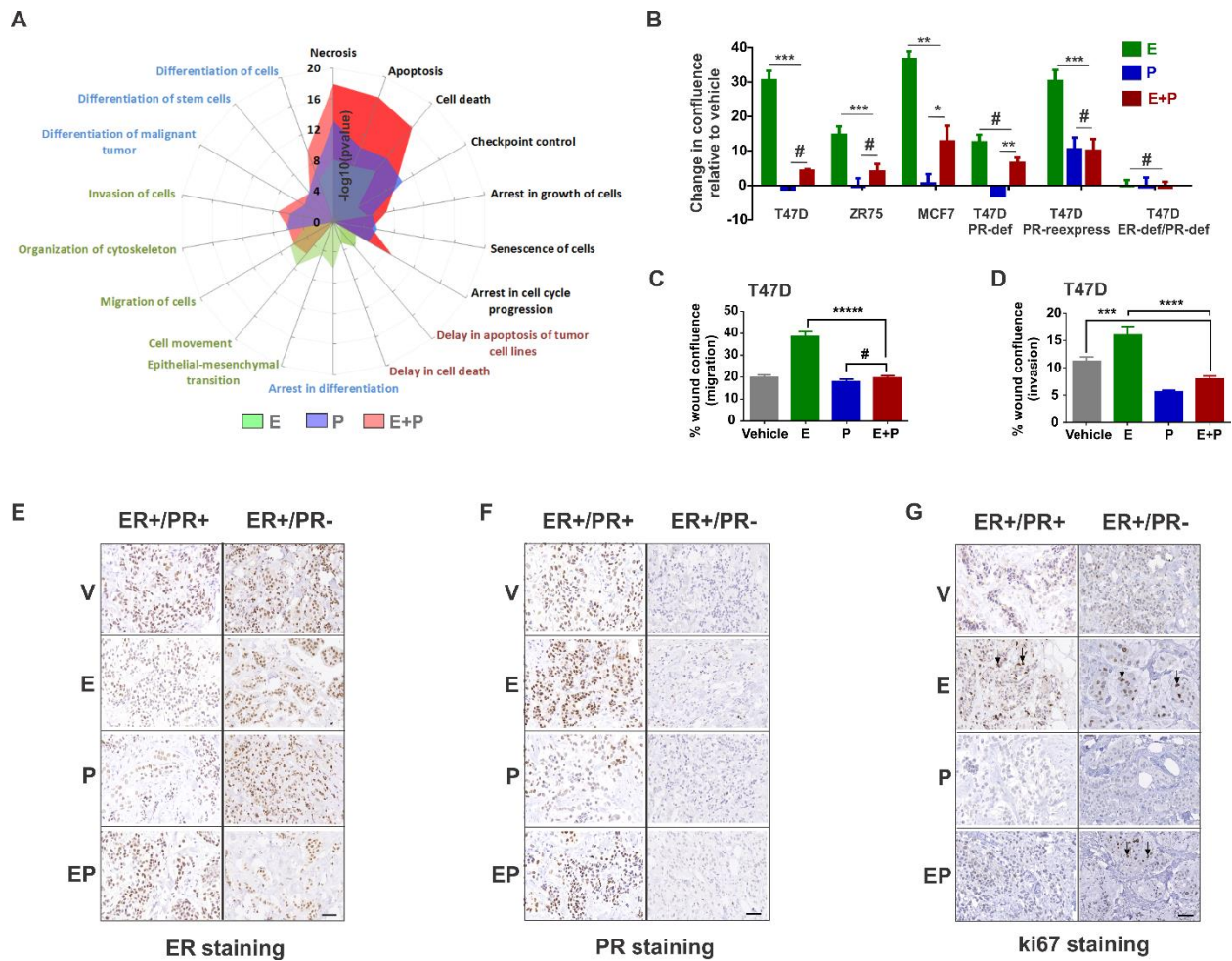


fig. S2. Progestin is a phenotypic antagonist of estrogen-induced cell proliferation, invasion, and migration. (A) Cellular pathways enriched in E, P and E+P regulated transcriptomes. Differential enrichment of functional pathways is visualized by plotting negative log of p value. P values measure the likelihood of association between the genes of interest and the functional pathway that can be due to random chance. (B) Cell confluence of various ER+/PR+ and ER+/PR-deficient cell models treated with E, P or E+P. (C) Migration and (D) matrigel invasion of T47D cells in response to treatment with E, P or E+P. (E - G) (E) Anti-ER and (F) anti-PR immunohistochemistry to determine ER and PR levels in patient tumors. (G) Representative images of changes in proliferation as measured by Ki67 staining of PR+ and PR- tumor explants treated ex-vivo with V, E, P or EP (scale = 200 μ m). Cell confluence, invasion and migration assays were done as three independent

experiments (>6 technical replicates per experiment). One of the three biological replicates is plotted. (* <0.05, ** <0.005, *** <0.0005, # not significant)

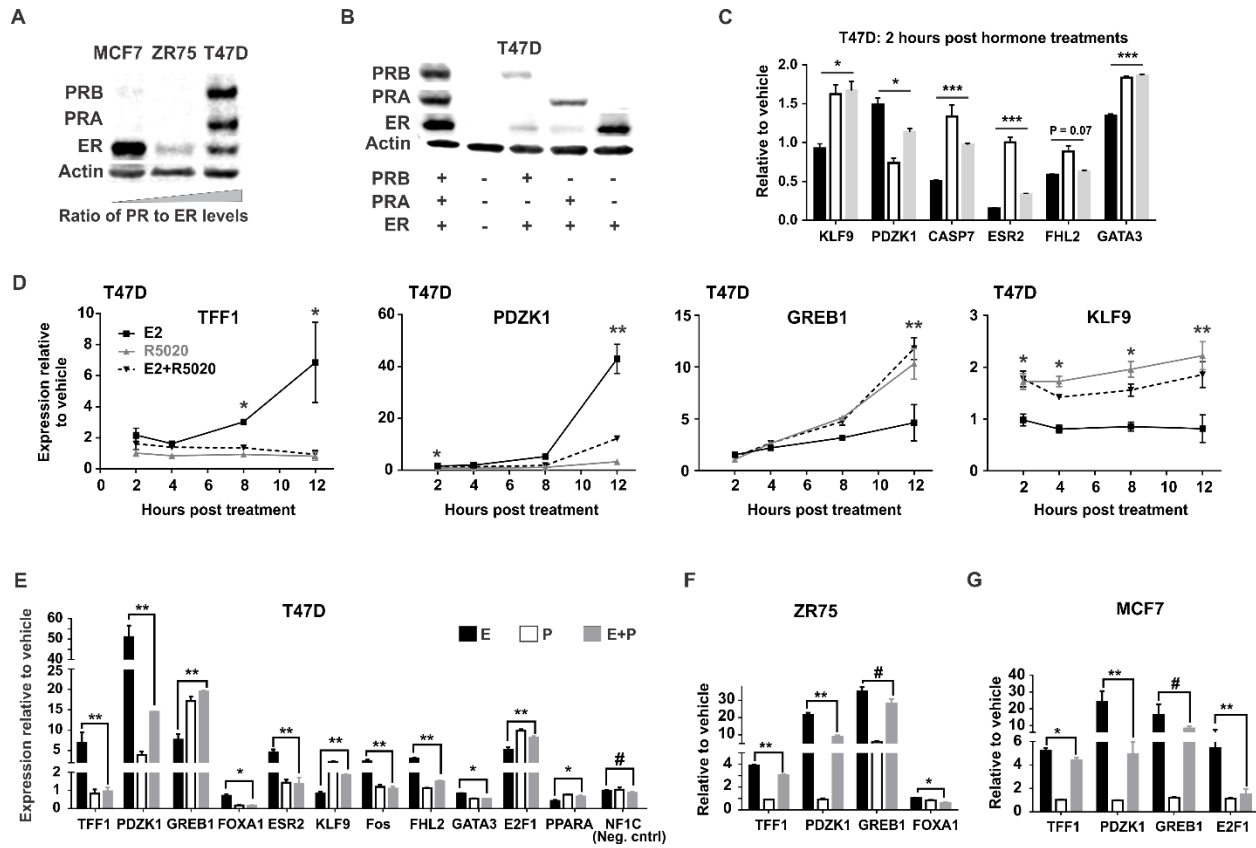


fig. S3. Progestin modulates estrogen-regulated gene expression. (A) ER and PR protein levels in T47D, ZR75 and MCF7 cells. **(B)** ER and PR levels in T47D cells and its derived sublines that lack either PR or both ER and PR. **(C)** For primary responders to estrogen treatment, progestin modulates estrogen-induced gene expression in T47D post two hours of hormonal treatment. **(D)** Two, four, eight and twelve hours' time course to study modulation of estrogen-regulated gene expression by progestin in T47D cells. **(E - G)** Progestin modulates estrogen-induced gene expression in **(E)** T47D, **(F)** ZR75 and **(G)** MCF7 cells. Fold change over vehicle treatment is shown. All RT-PCR experiments were done in triplicates. Mean and S.E.M of biological replicates is plotted. (* <0.05, ** <0.005, *** <0.0005, # not significant)

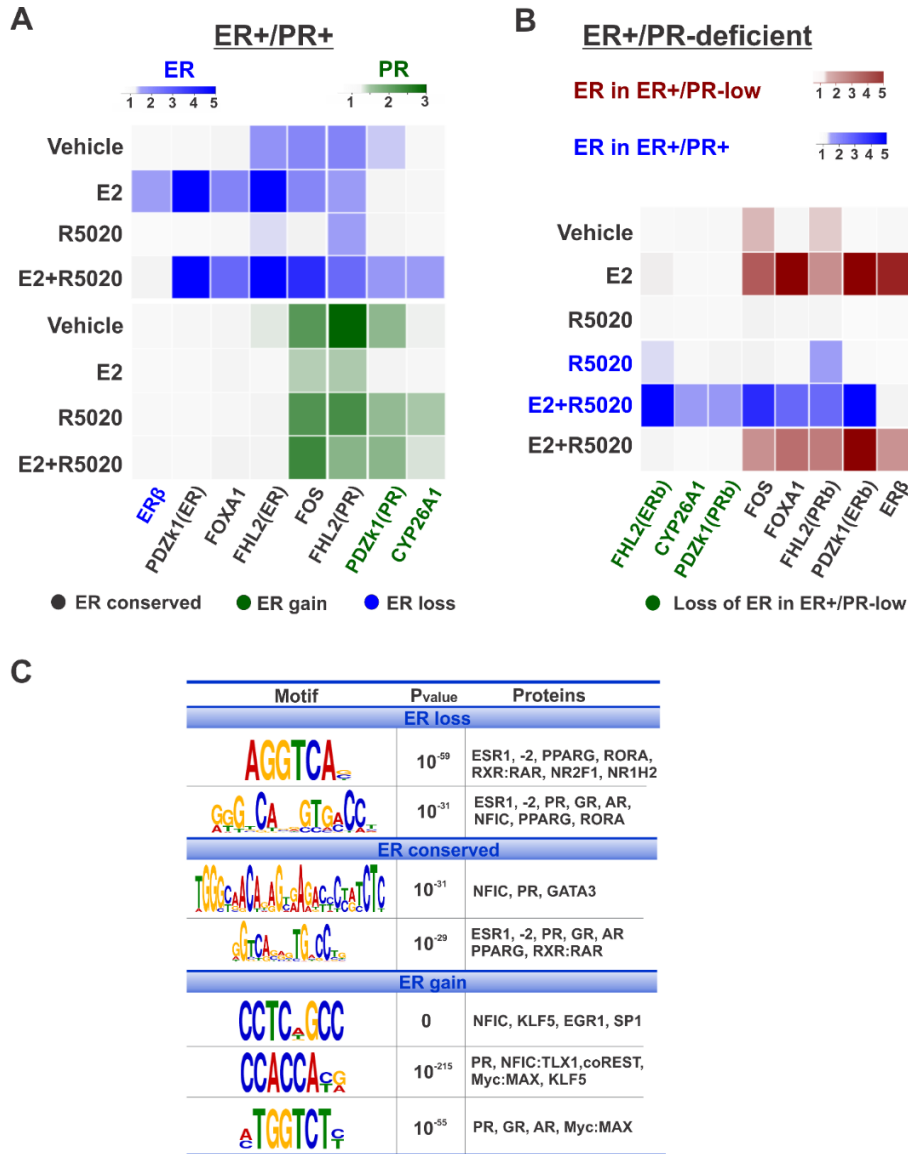


fig. S4. PR redirects ER to sites enriched for motifs of PR and PR-associated cofactors. (A - B) Heatmaps summarize ChIP-qPCR for **(A)** ER (blue) and PR (green) binding in T47D cells and **(B)** ER binding in PR-deficient T47D cells (red). ER binding sites that are conserved (black), lost (blue) or gained (green) after reprogramming by PR are shown. **(C)** Transcription factor binding motifs enriched in ER binding sites that are lost, conserved or gained due to reprogramming by PR. The significance of the enriched motif is reported by p value. The adjacent column lists proteins that potentially bind to the identified binding motifs. All ChIP-qPCR experiments were done in triplicates. Mean of three biological replicates is plotted.

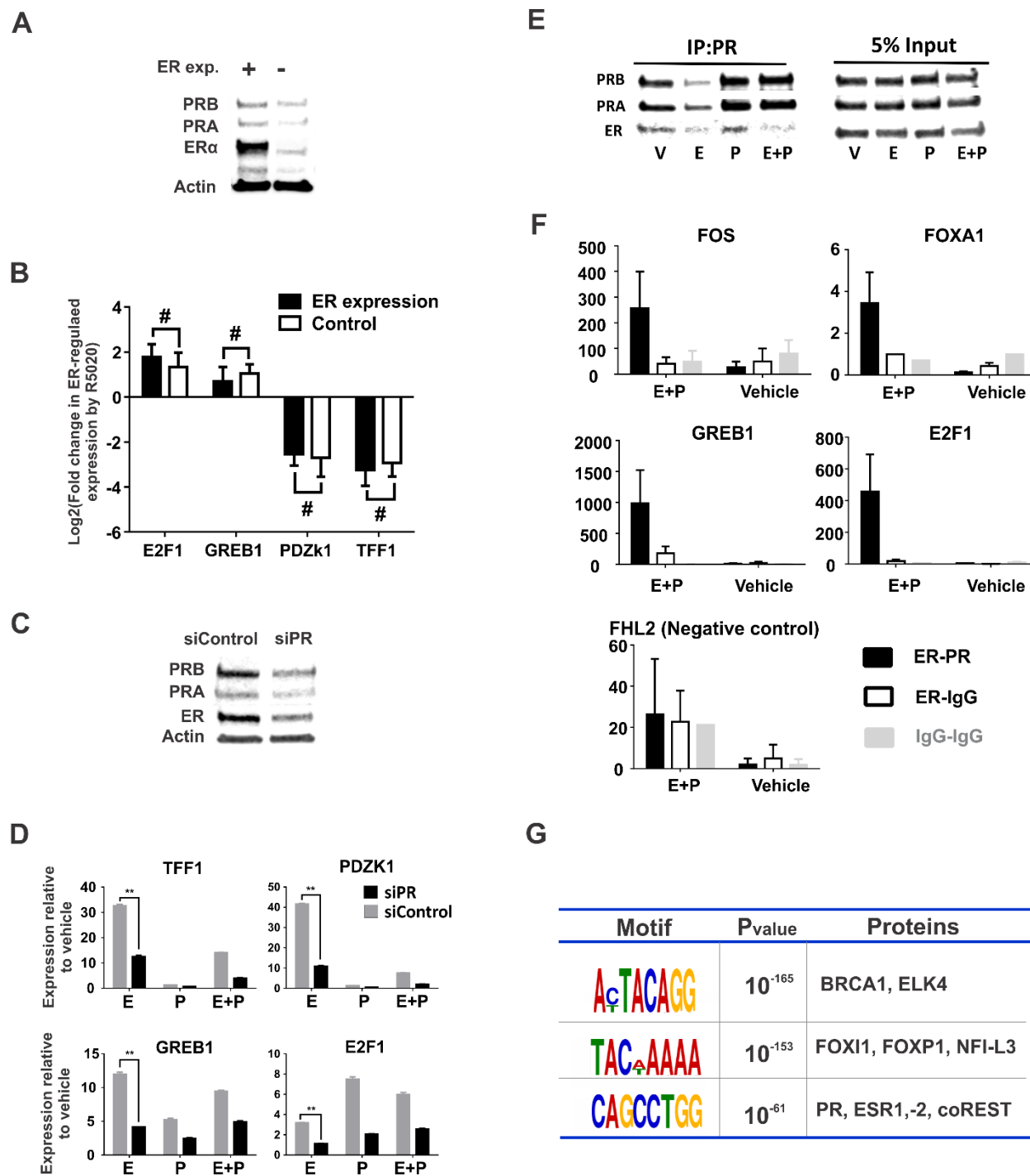


fig. S5. Noncompetitive interactions between ER and PR. (A) Immunoblot showing exogenous expression of ER protein in T47D cells. Expression of empty vector was used as a control. **(B)** Comparison of the effect of ER or control expression on modulation of estrogen-regulated gene expression by progestin. **(C)** Immunoblot of

lysate from T47D cells after siRNA specific depletion of PR or non-targeting control. **(D)** Gene expression in T47D cells treated with E, P or E+P after moderate knockdown of PR. **(E)** Anti-PR immunoprecipitation followed by immunoblotting for both ER and PR in T47D cells treated with different hormones. **(F)** ReChIP-PCR of anti-ER followed by anti-PR or control anti-IgG ChIP. **(G)** Transcription factor binding motifs enriched in binding sites for ER/PR complexes. The significance of the enriched motif is reported by p value. The adjacent column lists proteins that potentially bind to the identified motifs. ReChIP-PCR and RT-PCR was done as three independent experiments (three technical replicates per experiment). Mean and S.E.M of three biological replicates is plotted. (* <0.05, ** <0.005, *** <0.0005, # not significant)

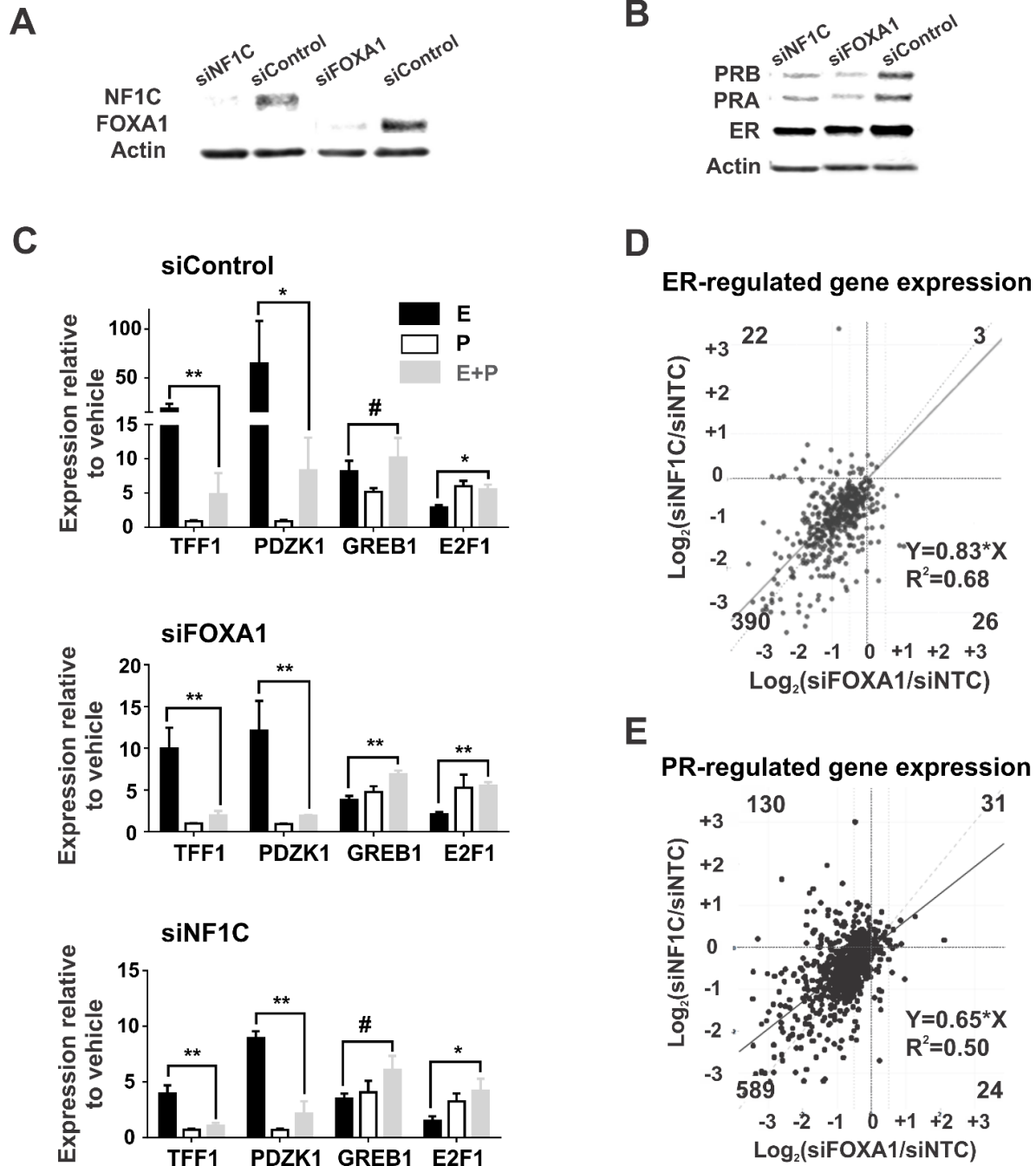


fig. S6. Depletion of FOXA1 or NF1C insignificantly impacts the effects of PR on ER-regulated gene expression. (A) Immunoblots of lysate from T47D cells after siRNA specific depletion of FOXA1, NFIC or non-targeting control. (B) Immunoblots to study the effect of FOXA1 and NFIC knockdown on the protein levels of ER and PR. (C) Neither FOXA1 nor NF1C is required for the effects of PR on ER-regulated gene

expression. Gene expression in T47D cells treated with different hormones after depletion of FOXA1, NF1C or non-target control. **(D, E)** Knockdown of FOXA1 or NF1C significantly impacts **(D)** ER and **(E)** PR regulated gene expression. Log fold change in gene expression on siFOXA1 and siNF1C compared to siControl is plotted. The effect of NF1C knockdown on ER and PR regulated gene expression is similar to the effect of FOXA1 knockdown. Linear regressions to compare the effects of FOXA1 and NF1C knockdown are plotted. RT-PCR was done as three independent experiments (three technical replicates per experiment). Mean and S.E.M of biological replicates is plotted. (* <0.05, ** <0.005, *** <0.0005, # not significant)

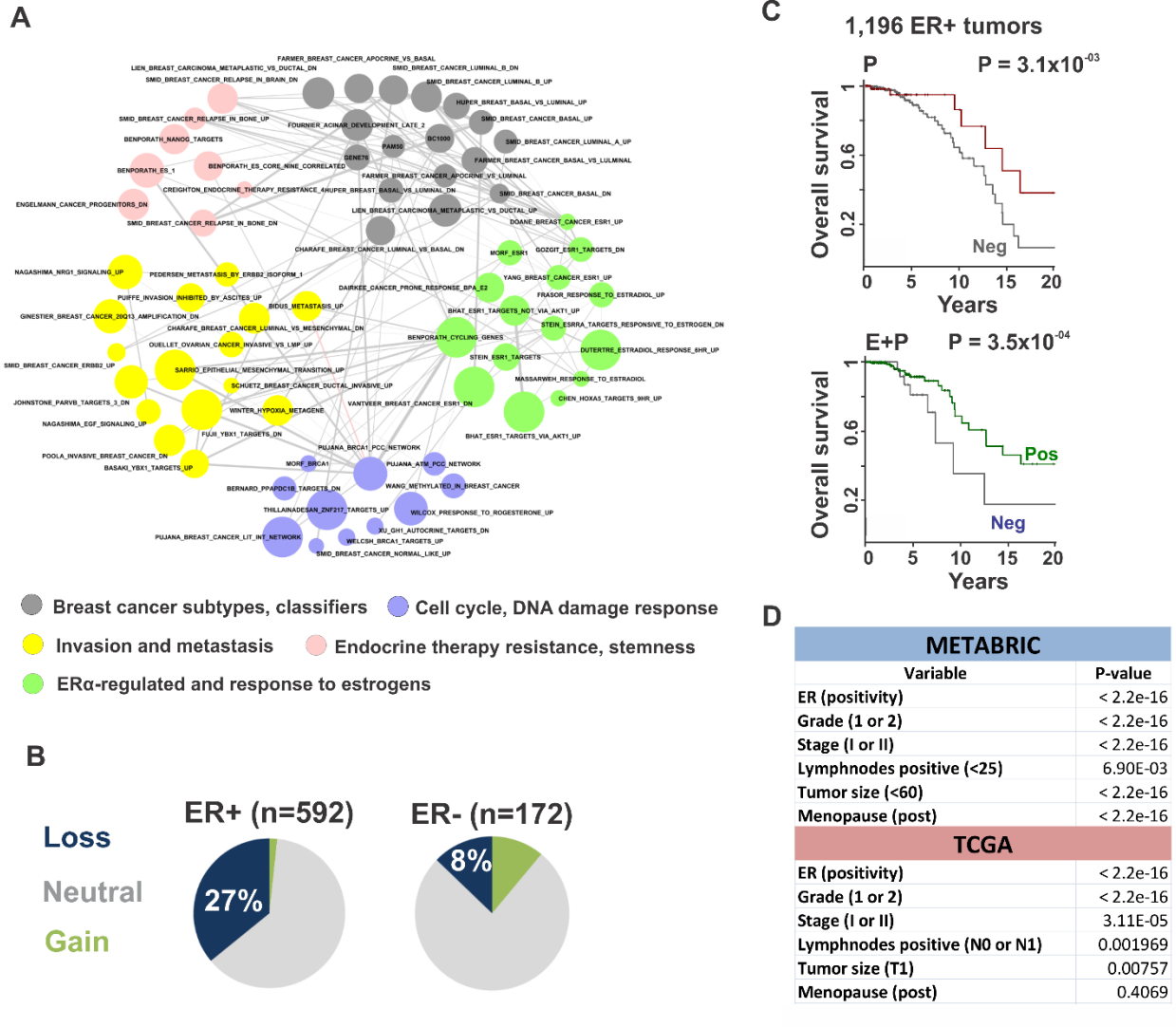


fig. S7. PR-regulated genes are enriched for breast cancer signatures, and PR contributes to the prognostic value of ER. (A) Network of functional modules enriched in PR-regulated genes. Each node represents a breast cancer signature annotated with its MsigDB identifier. The node size is inversely proportional to the bonferroni adjusted p-value and the edge width correlate with the overlap size of the enrichment between the functional modules. The enriched gene signatures are curated in five categories. **(B)** Frequency of copy number variation of PR gene locus in TCGA cohort categorized based on ER-positivity. **(C)** Overall survival in TCGA cohort classified by positive or negative correlation to PR-regulated signature scores. Curves are presented for progesterin scores in the absence (red) and presence (green) of estrogen. **(D)** Associations between positive tumor PR staining and favorable

clinicopathological variables in METABRIC and TCGA patient cohorts. P values are determined by chi-square test.